

Switching dynamics between metastable ordered magnetic state and nonmagnetic ground state

- A possible mechanism for photoinduced ferromagnetism -

Masamichi Nishino, Kizashi Yamaguchi

Department of Chemistry, Graduate School of Science,

Osaka University, Toyonaka, Osaka 560, Japan

Seiji Miyashita

Department of Earth and Space Science, Graduate School of Science,

Osaka University, Toyonaka, Osaka 560, Japan

Abstract

A statistical mechanical model for the switching mechanism of photoinduced magnetization is proposed making use of dynamics of magnetization in the circumstance with the metastable structure. As a typical model with metastability, the equilibrium and nonequilibrium properties of the Blume-Capel (BC) model have studied. We demonstrate reversible changes of magnetization corresponding to the change of system parameters, which would model the reversible photo-induced magnetization.

I. INTRODUCTION

Past decade reversible photo-induced magnetization has drawn much attention [1–4]. Very recently O. Sato, *et al.* have found that magnetic properties of prussian blue analogs, $K_{0.2}Co_{1.4}[Fe(CN)_6] \cdot 6.9H_2O$ [3] and $K_{0.4}Co_{1.3}[Fe(CN)_6] \cdot 5H_2O$ [4], can be switched between ferrimagnetic and paramagnetic states by visible and near-IR light illumination. The re-

versible changes of magnetization by magnetic field, electric field, and other external field have much attracted us because of not only academic interest but also the utility for applications in devices.

In this paper, we propose a statistical mechanical model which can show the reversible magnetic switching making use of the metastability of the order parameter. We consider a model whose ground state is nonmagnetic and the true thermodynamic state is paramagnetic but which has a rather stable metastable ferromagnetic state as an excited state.

Here, we adopt the Blume-Chapel (BC) model, which is a ferromagnetic $S = 1$ Ising model ($S^z = \pm 1$ or 0) with a crystal field splitting for easy-planar symmetry. The BC model is originally proposed to study first-order magnetic phase transitions [5,6]. Modeling the above mentioned mechanism, the spin at the site S_i represents the magnetic state ($S_i = \pm 1$) or nonmagnetic state ($S_i = 0$) on each site. In realistic materials the situation should be more complicated, but we choose this model as the simplest one which provides essential mechanism for the reversible magnetic switching.

When light radiate to materials, we generally expect that their physical properties change. The Kerr effect is a typical example, where the refractive index changes. Thus here we consider that the parameters of the model change according to the frequency of the light. In the equilibrium state, the physical properties must be unique functions of the system parameters. However, if the system has metastable states beside the equilibrium state, the system shows a kind of hysteresis phenomena, which gives a key mechanism of switching. The metastability is associated with the first order phase transition. Making use of the metastability of the BC model, we propose a mechanism of switching between ferromagnetic state and paramagnetic state by the change of parameters of the system which is expected by the light irradiation.

We will demonstrate the dynamics of magnetization corresponding to the reversible switching in the simulation for the proposed mechanism. We predict various features of the switching in the present mechanism, such as, the relation between the magnetization during the light irradiation and the state after the irradiation.

According to the effective parameters of the system during the irradiation, the state after irradiation is determined to be magnetic or nonmagnetic, which provides an essential mechanism of the reversible switching. However, if the effective parameters take intermediate values, the state after the irradiation becomes very stochastic. Namely, the switching to an desired state may fail with some probability. This uncertainty of the switching is also studied.

In Sect. II, we study the thermodynamic properties of the BC model and the nature of the metastability of the model. In Sect. III, a mechanism of the reversible switching is proposed. Summary and discussion are given in Sect. IV.

II. THERMODYNAMIC PROPERTIES OF THE BC MODEL

A. Model and phase diagram

In this section we study the thermodynamic properties of the BC model and the nature of the metastability of the model. The hamiltonian is given by

$$\mathcal{H} = -J \sum_{\langle i,j \rangle} S_i S_j + D \sum_i S_i^2. \quad (1)$$

where J is the exchange constant and D is the crystal field splitting. S_i takes on the values of $\pm 1, 0$ and $\langle i,j \rangle$ indicates that the summation is over all nearest-neighbor pairs on a lattice. In the present paper we study the model on the simple cubic lattice with the linear dimension L . We deal with ferromagnetic interaction ($J > 0$) and positive D .

Thermodynamic properties of the BC model have been studied extensively, *i.e.* the model including the extended BC model have been studied by mean-field approximation [5–7], renormalization [8–10], Monte Carlo methods [11,12], *etc* [13]. In particular, the tricritical point of the model between the second order transition line and the first order transition line has been investigated by various method [14–17]. In Fig. 1 we depict the phase diagram in (D, T) plane. There, circles are determined by Monte Carlo simulations. The closed circles are determined from the cross point in the Binder plot of the magnetization [18] and we find the phase transitions there are of the second order. The open circle shows a

first-order phase transition point. In order to determine a critical temperature of the first-order phase transition, we use the following simplified method, although there are several methods to determine the first order phase transition point making use of histogram of the order parameter [19]. First we look for the hysteresis: We perform a simulation with a disordered initial state reducing the temperature gradually, and find a temperature, (say, T_L), at which the system jump to the ordered state. Then we performed another simulation with a complete ordered state at a low temperature and increase the temperature gradually to find a temperature (T_H) at which the system jumps to the disordered phase. If T_L and T_H are separated significantly, then we regards the phase transition is of the first order. In order to determine the critical temperature we performed the following simulations: We prepare an initial configuration half of which is the ordered state and the other half is disorder. We perform Monte Carlo simulations with different sequences of random numbers (in most cases we used 30 samples). If the all samples reach to the ordered phase, then we regard the set of the parameters (D, T) belongs to the ordered state. On the other hand if the all samples reach the disordered phase, then it is regarded as the disordered state. If the samples distribute among both phase, we regard the case as the critical region. The error bar in Fig. 1 shows the maximum range of the critical region and the open circle is put in the middle of the region. This procedure has been done for $L = 10$. If we increase the size of the system the error bar would shrink. However for the purpose of the present paper, we need only rough phase diagram and Fig. 1 is satisfactory.

The triangle shows the position of the tricritical point obtained by M. Deserno [17], which locates consistently in Fig.1.

B. Metastability of the BC model

As has been mentioned in the introduction, the BC model has metastable structure. First we investigate the free energy obtained by a mean-field approximation as a function of the magnetization:

$$F(M) = -K_B T \log[\text{Tr} \exp(-\beta \mathcal{H}_{\text{MF}}(M))] - \frac{1}{2} \beta J z M^2 \quad (2)$$

with

$$\mathcal{H}_{\text{MF}}(M) = zJMS - DS^2. \quad (3)$$

where β is $1/K_B T$, z is coordination number and M is mean magnetization per site. For the simple cubic lattice, $z = 6$. The free energy is explicitly given by

$$F(M) = -K_B T \log[2 \exp(-\beta D) \cosh(\beta J z M) + 1] - \frac{1}{2} \beta J z M^2. \quad (4)$$

Hereafter we take J as a unit of energy and also we put $K_B = 1$. For $D = 1.0$ and $T = 4.0$ in the paramagnetic region (large T), $F(M)$ has a single minimum (Fig. 2(a) for $D = 1.0$ and $T = 4.0$). If D is small the system shows the second-order phase transition and $F(M)$ has double minima (Fig. 2(b) for $D = 1.0$ and $T = 1.2$). On the other hand if D is close 3, then the system shows the first order phase transition and $F(M)$ has 3 minima; for $D > 3$ nonmagnetic state is the true equilibrium state (Fig. 2(c) for $D = 3.2$ and $T = 1.0$), and for $D < 3$ ferromagnetic state is the true equilibrium state (Fig. 2(d) for $D = 2.8$ and $T = 1.2$). If D is large the system is nonmagnetic for all temperature and $F(M)$ has a single minimum.

In Fig. 3, we show a phase diagram including metastable region in the mean field free energy (4). For D which is smaller than that at the tricritical point (D_t, T_t) , the shape of the free energy changes as Fig. 2(a) (the paramagnetic region, hereafter we refer this region as I.) \rightarrow Fig. 2(b) (an ordered state with bistability, region II) \rightarrow Fig. 2(d) (an ordered state with a metastable paramagnetic state, region III). The tricritical point (D_t, T_t) is obtained as $(2.7726, 2.0)$ [7] and plotted by a triangle in Fig. 3. The boundary between I and II is an phase transition line in the equilibrium, which is the second order phase transition. This is shown by a solid line. On the other hand the boundary between II and III does not correspond to any equilibrium phase transition but it shows a point where the metastability appears. This boundary is shown by a dash-dotted line. At these lines the coefficient of M^2

of $F(M)$ vanishes. These lines join at a point Q , $(D_Q, T_Q) = (2.7783, 1.899)$, the value of D is larger than D_t .

For $3 > D > D_Q$, the shape of the free energy changes as Fig. 2(a) \rightarrow Fig. 2(c) (a paramagnetic state with a metastable ferromagnetic state, region IV) \rightarrow Fig. 2(d). The boundary between I and IV is a point where the metastability appears, which is shown by a dotted line. The boundary between III and IV is the first order phase transition in the equilibrium, which is shown by a dashed line.

As shown in the inset in Fig. 3, between D_t and D_Q , a complicated change of the shapes of $F(M)$ occurs: (a) \rightarrow (c) \rightarrow (d) \rightarrow (b) \rightarrow (d).

For $D > 3$, only the boundary (dotted line) for the metastability exists.

Second, we performed simulations with a complete ferromagnetic initial configuration and count how many samples decay to the disordered phase with in 10,000, 100,000 and 1,000,000 Monte Carlo Steps (MCS) in the system of $L = 10$ and 20 with the periodic boundary condition.

In Fig. 4, we plot the highest temperature at which more than 2/3 of samples ($L=10$ and 30 samples) remain ferromagnetic state ($|\sum_i S_i| > 0.5L^3$) by upward triangles (10,000MCS), circles (100,000MCS) and downward triangles (1,000,000MCS). Here we find that the transition region between simple paramagnetic region and metastable region is rather narrow and we can distinguish the region of metastable state rather clearly. The data for 1,000,000 MCS shows a sharp change near $D = 4.0J$. In the inset of Fig. 4, the number of samples which remain ferromagnetic are shown, where we find rather wide range of the transition region.

Here, we investigate the boundary of the metastability of the complete ferromagnetic state from a view point of local nucleation process. Let us consider configurations with a cluster of nonmagnetic sites. The energy difference between the complete ferromagnetic state and a state with a cluster, say ΔE , is given by

$$\Delta E = -nD + mJ \quad (5)$$

where n is the number of nonmagnetic sites and m is the number of exited bonds (*i.e.*, $S_i S_j = 0$) which have spin 0. In Fig. 5(a) the excess energy, ΔE , of configurations with a cluster of nonmagnetic sites are shown. We found easily that the complete ferromagnetic state is unstable even for a flip to a single nonmagnetic site when $6J < D$. Thus the upper limit of the metastability locates at $D = 6J$. For $3J > D$, the ferromagnetic state becomes true equilibrium state. Thus the metastable ferromagnetic state exists in the range $3J < D < 6J$, consistently with the above investigations. At a given value of D in the range, the excess energy of a cluster configuration, ΔE , increases as n increases for small values of n . Against fluctuation with such clusters the complete ferromagnetic state is locally stable, (*i.e.* metastable). On the other hand for large values of n , ΔE decreases when n increases. This means that once the cluster of nonmagnetic sites appears it grows and the ferromagnetic state is destroyed. Between these two region, ΔE has maximum. In Fig 5(b) ΔE for the most compact cluster is plotted as a function of n for various values of D .

The configuration for the maximum ΔE is called critical nucleus and n at this configuration is named n_C . The boundary of the metastability could be given

$$e^{-\beta\Delta E(n_C)} \simeq p_{\min}, \quad (6)$$

where p_{\min} is the smallest nucleation rate which is detectable in the observation (in Monte Carlo simulation in the present case).

Because we are studying phenomena in the time scale $t < 10^6$ MCS and the size of system $L^3 \simeq 10^3$, $p_{\min} \simeq 10^{-9}$.

Because we are interested in the temperature region, $T < 0.5$, only the phenomena with ΔE of

$$\Delta E < 10J \quad (7)$$

is meaningful in the present observation because

$$e^{-\beta\Delta E} > p_{\min} \simeq 10^{-9}. \quad (8)$$

For $D > 4J$, the ferromagnetic state is stable only against clusters with a few nonmagnetic sites. Thus the region of metastability exists only $T \ll 1$. In the range ($\Delta E < 10J$) we find that the $\Delta E(n)$ becomes very flat at $D \simeq 4$. Thus we expect that the boundary of the metastability becomes ill defined for this case, which would give the explanation of the wide range of the transition observed in Fig. 4.

In the same way, we determine the metastable region for the disordered phase which are also shown in Fig. 4 ($D < 3$), by boxes (10,000MCS) and diamonds(100,000MCS). Qualitatively, the phase diagram in Fig. 4 agrees well with that of Fig. 3. If we look at Fig. 4 carefully, the boundary corresponding to the second order phase transition line in Fig. 1 (dotted line) shifts to low temperature side. This disagreements is simply due to the definition of the boundary in Fig. 4. The boundary in Fig. 4 are obtained as the highest temperatures at which the system does not have the magnetization below $M = 0.5N$ during the simulation. Thus if the equilibrium spontaneous magnetization $M_s(T)$ is less than $M = 0.5N$, the temperature T belongs the right hand side region of the boundary (T is higher than the boundary), although it is smaller than the phase transition point $T_C(D)$. Furthermore, even if the equilibrium magnetization is larger than $M = 0.5N$, the system can have the magnetization of $M < 0.5N$ as the fluctuation. Thus the boundary of the present criterion locates in the low temperature side of the true phase boundary.

In the present model the spontaneous magnetization M_s changes very rapidly with the temperature and the point of $M_s = 0.5N$ is very close to the phase transition point (see Appendix). Thus the difference discussed above is mainly due to the latter reason. Actually if we obtain the boundary in the system of $L = 20$ it is found to locate more close to the phase transition point.

Next we study the size dependence of the metastability of ferromagnetic state. We expect the metastable state in the present model is in so-called stochastic region or single nucleation region [20]. There we expect the nucleation rate in the whole volume is about 8 times larger in the system of $L = 20$, because the volume of the system of $L = 20$ is 8 times larger than that for $L = 10$. Actually in the cases with $D >$ about 2.9, we observe the marginal points

for 12,500MCS (the symbol \times in Fig. 4) and 125,000MCS (the symbol $+$ in Fig. 4) of the systems of $L = 20$ well overlap with those for 100,000 and 1,000,000 in the system of $L = 10$.

III. REVERSIBLE SWITCHING

In this section we consider a possible mechanism of switching between the ordered state and disordered state, making use of the structure of metastability studied in the previous sections. We consider a system which is nonmagnetic in the equilibrium state but it has a fairly stable metastable ordered state. We can find such system in the BC model with D a little bit larger than 3.0 at low temperature. We take a point A ($(D, T) = (3.2, 0.6)$) as such a point (see Fig. 6). Here simulations are done in a system of $L = 10$. We have checked that qualitative natures do not change in the system of $L = 20$ and even quantitatively most behavior is reproduced in the system of $L = 20$.

If we start with a high temperature ($T = 1.5$) and cool down the system, we find a paramagnetic state at A. On the other hand if we start with complete ferromagnetic state at $T = 0$ and warm up the system we find a ferromagnetic state at A. At this point let us consider a mechanism of the reversible switching. If the system is put in other environments, such as under light irradiation, the parameters of the system, $J/k_B T$ and $D/k_B T$, would be renormalized. Generally we expect that both $J/k_B T$ and $D/k_B T$ will become smaller. Let a point X (D_X, T_X) for such renormalized state. Now we study the change of magnetization after the change of the parameters $A \rightarrow X \rightarrow A$. Here let us take D_X to be 2.8. If T_X is in the ordered state and above the temperature where the metastability exists, then the system becomes ferromagnetic rapidly after the system move to X. After the system come back from X to A, the system is trapped in the metastable state. As an example of such T_X we take $T_X = 1.25$ and the change of magnetization is shown in Fig. 7. Hereafter we call the point B; $(D_B, T_B) = (2.8, 1.25)$. There we repeat the process ($A \rightarrow B \rightarrow A \rightarrow B \dots$) in order to check the stability of the dynamics. Here simulations were performed as follows: First we simulate the system at a high temperature $T = 1.5$ with 50000MCS and

then gradually reduce the temperature by $\Delta T = 0.1$ iteratively. At each temperature 50000 MCS are performed. Next the system moved to the point B and 20,000MCS is performed. Then the system comes back to A and stays there for another 100,000MCS. There we find that the system is always the metastable ferromagnetic state when it comes back from the point B. On the other hand if T_X is high ($T_B = 1.5$), the system is disorder. This point will be called C; $(D_C, T_C) = (2.8, 1.5)$. The change of magnetization is shown in Fig. 8, where the system at point A is always paramagnetic.

Whether the state after the system come back from X is ferromagnetic or paramagnetic depends on the temperature T_X . For intermediate temperature, this state distributes among ferromagnetic or paramagnetic state. For example the time evolution of the magnetization for $T_X = 1.38$ is shown in Fig. 9. We investigate reliability of the switching making use of the quantity:

$$P = \left(\frac{N_f - N_p}{N_f + N_p} \right)^2, \quad (9)$$

in continuous 10 times repetition, where N_f is the number of appearance of ferromagnetic state and N_p is as well for paramagnetic state. This quantity indicates the degree of certainty of the state after the system come back from X.

If a cluster of nonmagnetic sites is larger than the critical size (n_C), the state become nonmagnetic after the irradiation. The distribution of cluster of nonmagnetic sites at X ($p_X(n)$) determines the distribution of N_f . The quantitative analysis for $p_X(n)$ is difficult but we expect that $N_p/(N_f + N_p)$ is a monotonic function of T_X and is very small for small T_X and $N_f/(N_f + N_p)$ is also very small for large T_X . Thus we identify the three regions of T_X , *i.e.*, $N_p/(N_f + N_p) \simeq 0$ ($P = 1$), $0 < N_p/(N_f + N_p) < 1$ ($P < 1$) and $N_p/(N_f + N_p) \simeq 1$ ($P = 1$) rather clearly.

The average of P is shown in Fig. 10 estimated from four sets of $N (= N_f + N_p) = 10$ samples varing T_X from 1.2 to 1.5. We performed simulations for each T_X value with different random number sequences. In Fig. 10, P is almost 0 near $T=1.35$ and this range corresponds to the marginal point and large fluctuations are occured, while in the range of

stable ferromagnetic state $T \leq 1.25$ or of paramagnetic state $T \geq 1.45$, the switching is very deterministic, i.e. $P \simeq 1$ as is expected.

Let us now demonstrate the reversible switching. In order to realize reliable switchings we choose points B and C. Dynamics of magnetization are shown in Fig. 11, where reversible magnetization process is actually demonstrated. If the temperature at the point B becomes lower and the temperature at C becomes higher, the switching becomes more reliable.

In this demonstration, the point B and C correspond to state under irradiation. Here it would be supposed that two species of light which change the physical parameter at point A($D = 3.2, T = 0.6$) to B($D = 2.8, T = 1.25$) and C($D = 2.8, T = 1.5$).

As reported in experiment [3,4], light with shorter wave length was used for switching to the ferromagnetic state. Generally we expect that irradiation of short wave length cause large renormalization of the parameter, although the way of renormalization depends on the micro properties of the material. In the above demonstration, the use higher temperature for switching off the magnetization, which is intuitively not the consistent with the experiment. Thus we demonstrate the switching taking another point for C. Here we take the point C' at ($D = 3.1, T = 1.0$). It would be possible that the renormalized values of D and T shift from A to C' and to B corresponding to the frequency of the light. Dynamics of magnetization is shown in Fig. 12, where the reversible switching is demonstrated again.

IV. SUMMARY AND DISCUSSION

We investigated the metastable ferromagnetic region of the BC model by Monte Carlo method. The metastable ferromagnetic region actually exists and was found to be very steady. We observed dynamics of magnetization for variety of change between the parameters (D, T) . In the assumption that photon's effect causes renormalizations of (D, T) , we actually demonstrated reversible magnetic switching in choosing adequate sets of (D, T) .

So far the switching mechanism has been discussed with the picture of the adiabatic potential for the nonmagnetic ground state and excited state with magnetic moments of the microscopic structure. Such structure is the necessary condition for the reversible switching but not satisfactory condition. That is, even if the system becomes magnetic during the light irradiation the system does not necessarily stay ferromagnetic state after the irradiation. In order to have macroscopic change of state, the mechanism for macroscopic order parameter is necessary. In this sense, we propose a mechanism of the reversible photoinduced magnetization based on the metastability structure of the ferromagnetic state.

ACKNOWLEDGMENTS

The authors would like to thank Dr. Osamu. Sato for his kind discussion on the experiments. The present work was supported by Grant-in-Aid for Science Research from the Ministry of Education, Science and Culture of Japan.

APPENDIX A: THE SPONTANEOUS MAGNETIZATION

For 2D Ising model on the square lattice the spontaneous magnetization per spin is given by the famous C. N. Yang's solution [21]:

$$m_s = \left(1 - \left(\frac{1}{\sinh^2 2\beta J}\right)^4\right)^{1/8}. \quad (A1)$$

Here $K_B T_C/J = 2.269$ and $m_s = 0.5$ at $K_B T_{1/2}/J = 2.240$. The temperature for $m_s = 0.5$ is very close to T_C :

$$\frac{T_{1/2}}{T_C} = 0.987. \quad (A2)$$

The present model is three dimensional. The change of magnetization is milder than that of 2D because of the exponent β is about 0.32 instead of 1/8. However, it is still very steep, as shown in Ref. [22].

REFERENCES

- [1] A. Hauser, J. Adler and P. Gütlich, Chem. Phys. Lett. **152**, 468 (1988).
- [2] P. Gütlich, A. Hauser and H. Spiering, Angew. Chem. Int. Ed. Engl. **33**, 2024 (1994).
- [3] O.Sato, T.Iyoda, A. Fujishima, and K. Hashimoto, Science **272**, 704 (1996). @
- [4] O.Sato, Y. Einaga, T.Iyoda, A. Fujishima, and K. Hashimoto, J.Electrochem.Soc. **144**, L11 (1997).
- [5] M. Blume, Phys. Rev. **141**, 517 (1966).
- [6] H. W. Capel, Physica **32**, 966 (1966); **33**, 295 (1967); **37**, 423 (1967).
- [7] M. Blume, V. J. Emery, and R. B. Griffiths, Phys. Rev. A **4**, 1071 (1971).
- [8] G. D. Mahan and S. M. Girvin, Phys. Rev. B **17**, 4411 (1978).
- [9] A. Benyoussef, N. Boccara, and M. El Bouziani, Phys. Rev. B **34**, 7775 (1986).
- [10] N. S. Branco and B. M. Boechat, Phy. Rev. B **56**, 11673 (1997).
- [11] M. Tanaka and T. Kawabe, J. Phys. Soc. Jpn. **52**, 2194 (1985).
- [12] Y. Aoyama, W. Chen and M. Tanaka, J. Phys. Soc. Jpn. **66**, 272 (1997).
- [13] T. Kaneyoshi and J. Mielnicki, J. Phys.: Condens. Matter **2**, 8773 (1990) .
- [14] D. M. Saul, M. Wortis and D. Stauffer, Phys. Rev. B **9**, 4964 (1974).
- [15] A. K. Jain and D. P. Landau, Phys. Rev. B **22**, 445 (1980).
- [16] D. P. Landau and R. H. Swendsen, Phys. Rev. Lett. **46**, 1437 (1981).
- [17] M. Deserno, Phys. Rev. E **56**, 5204 (1997).
- [18] K. Binder, Z. Phys. **B43**, 119 (1981).
- [19] J. Lee and J. M. Kosterlitz, Phys. Rev. Lett. **65**, 137 (1990).

- [20] P. A. Rikvold, H. Tomita, S. Miyashita, and S. W. Sides, Phys. Rev. E **49**, 5080 (1994).
- [21] C. N. Yang, Phys. Rev. **85**, 808 (1952).
- [22] N. Ito and M. Suzuki, J. Phys. Soc. Jpn. **60**, 1978 (1991).

@

FIGURES

FIG. 1. The phase diagram of the BC model. The closed circles denote the second ordered phase transition obtained by a Monte Carlo simulation. The triangle denotes the tricritical point determined by M. Deserno. The open circle denotes the first order phase transition obtained by a Monte Carlo simulation. The errorbar denotes the region of the hysteresis.

FIG. 2. The mean field free energies of the BC model for various parameter sets (D, T) .

FIG. 3. The phase diagram including metastable region in the mean field theory (See text).

FIG. 4. The metastable ferromagnetic and paramagnetic region obtained by Monte Carlo method. The dashed line is the phase boundary shown in Fig. 1. The symbols denote the boundaries of the metastable region (For details, see text).

FIG. 5. (a) Clusters of n nonmagnetic sites and the energy difference (ΔE) from the completely ferromagnetic state. (b) Dependence of (ΔE) on the number of sites n for various values of D . Symbols $+$, ∇ , \times , \square , \bullet , \triangle , \diamond , and \circ denote data for $D=1, 2, 3, 3.5, 4, 4.5, 5$, and 6 respectively. The maximum point corresponds to the size of the critical nucleus for each value of D .

FIG. 6. Switching path in (D, T) plane with phase boundary and metastable regions. Definitions of A, B, C and C' are given in the text.

FIG. 7. The change for the second order moment of magnetization $\langle M^2 \rangle$ per site in the case of $T_X=1.25$.

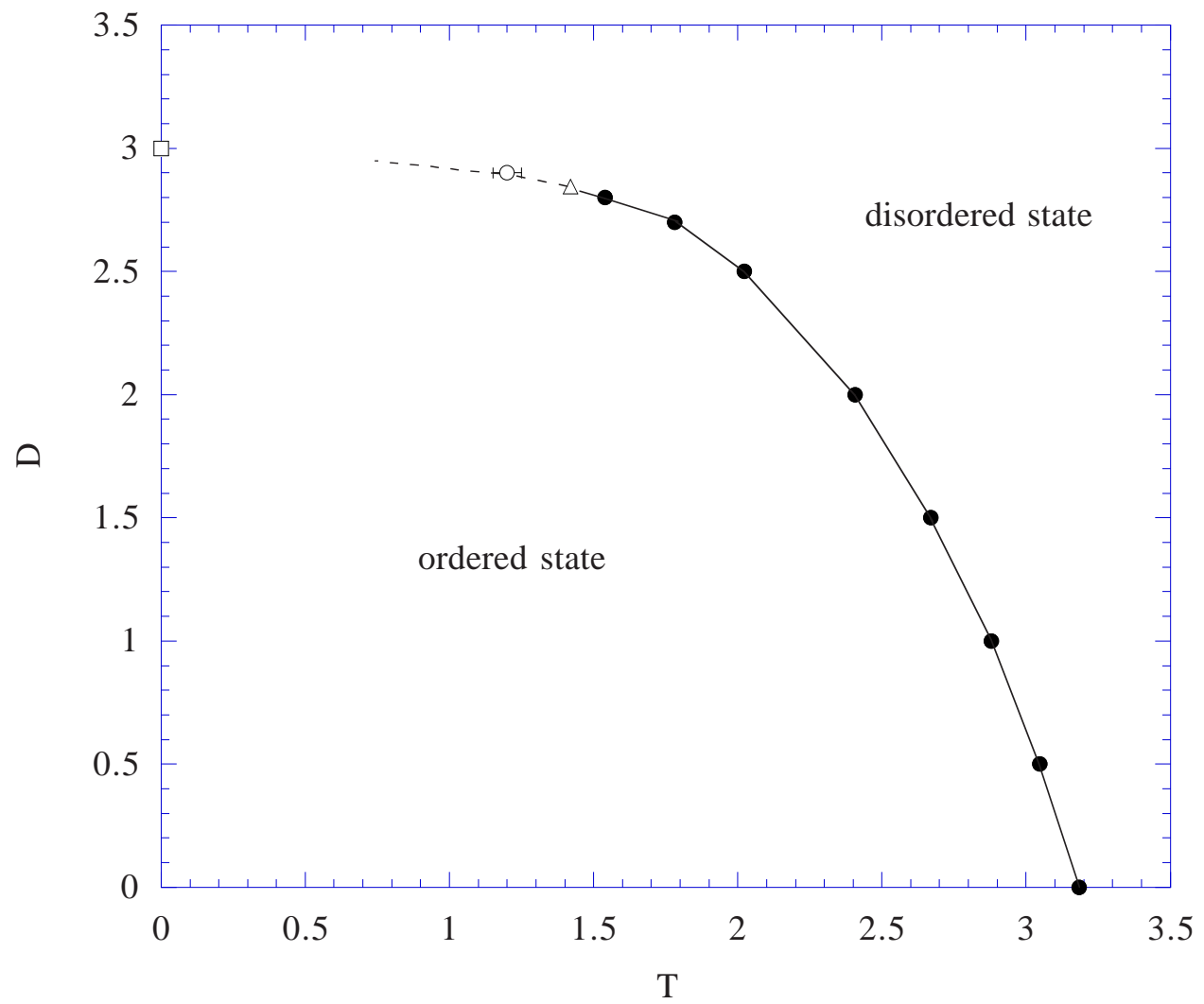
FIG. 8. The change for the second order moment of magnetization $\langle M^2 \rangle$ per site in the case of $T_X=1.5$.

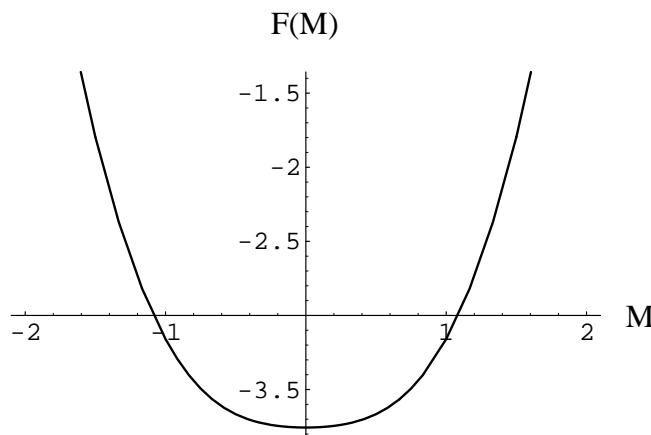
FIG. 9. The change for the second order moment of magnetization $\langle M^2 \rangle$ per site in the case of $T_X=1.38$.

FIG. 10. Average of the reliability P as a function of T_X for fixed $D_X=2.8$.

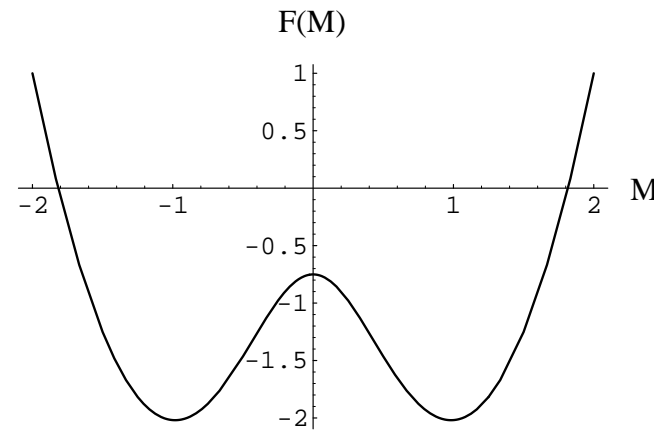
FIG. 11. The change for the second order moment of magnetization $\langle M^2 \rangle$ per site in the case of choosing B=($D = 2.8, T = 1.25$) and C=($D = 2.8, T = 1.5$).

FIG. 12. The change for the second order moment of magnetization $\langle M^2 \rangle$ per site in the case of choosing B=($D = 2.8, T = 1.25$) and C'=($D = 3.1, T = 1.0$).

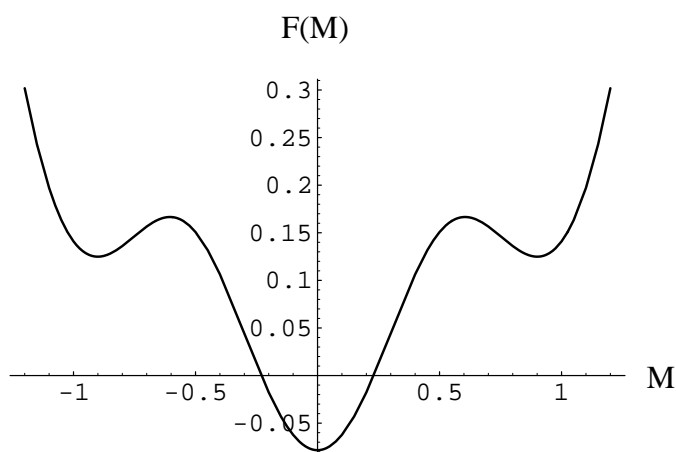




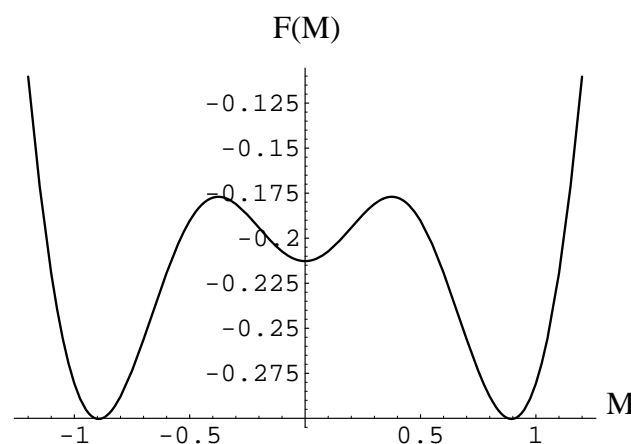
(a) $(D, T) = (1.0, 4.0)$



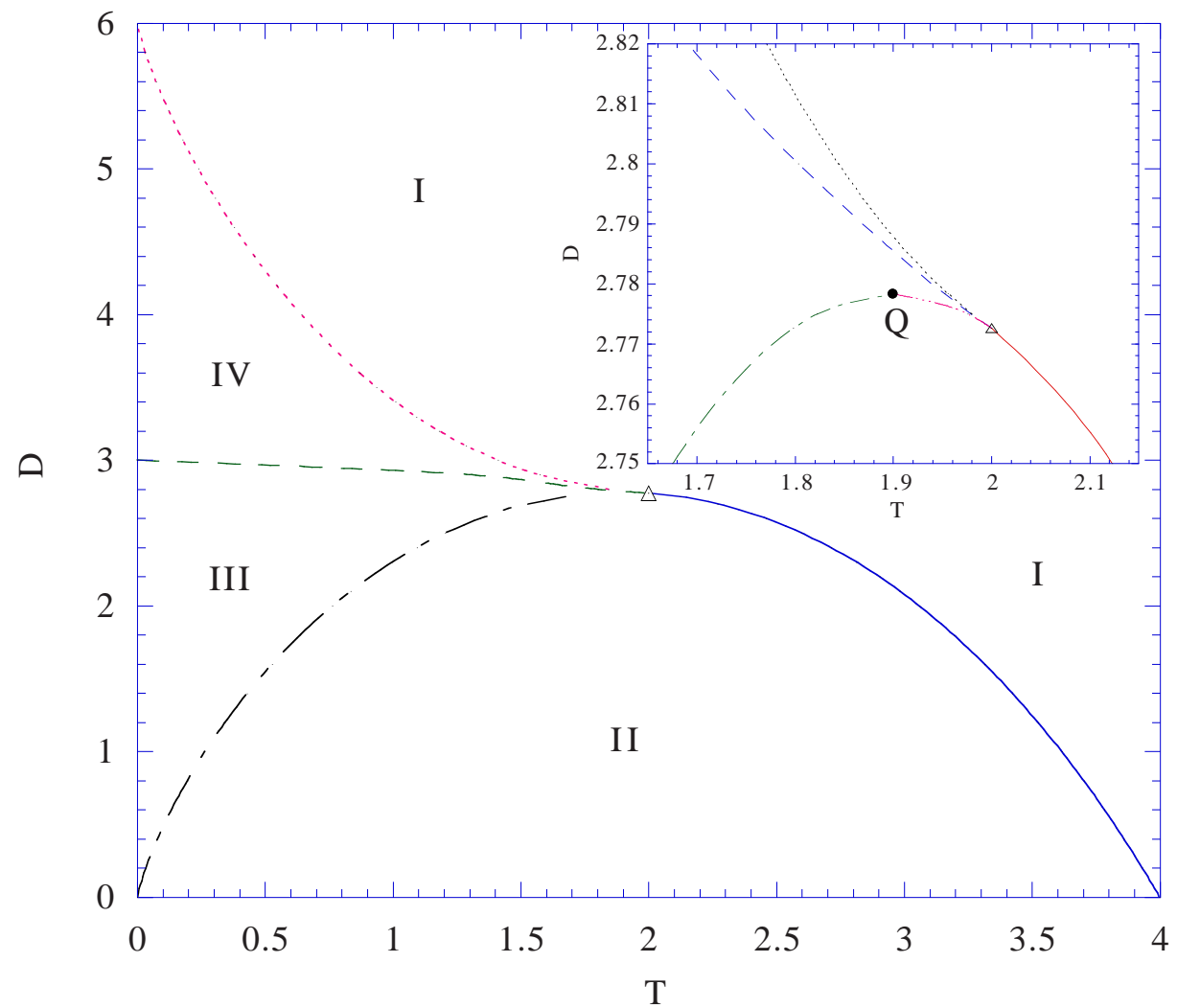
(b) $(D, T) = (1.0, 1.2)$

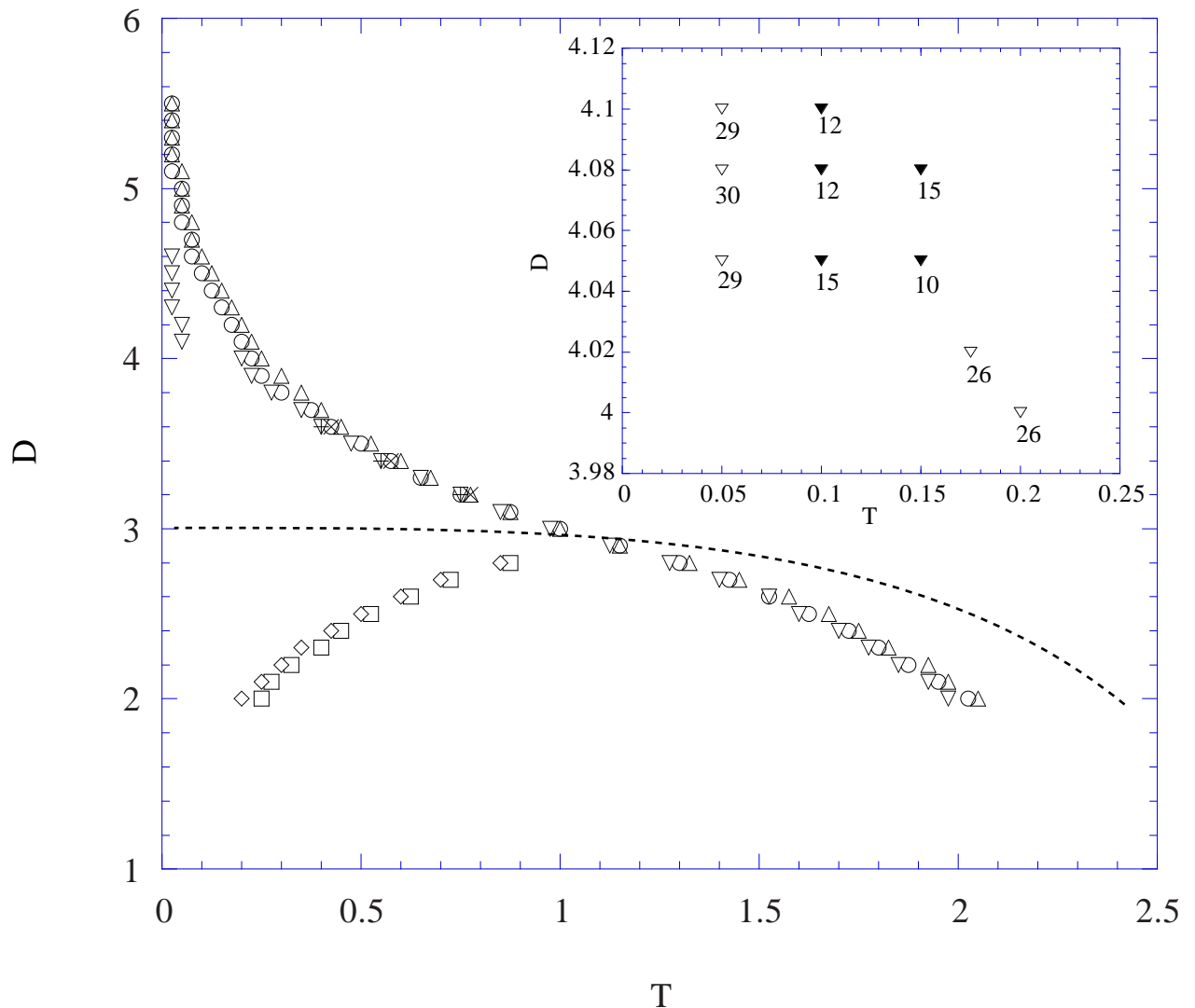


(c) $(D, T) = (3.2, 1.0)$



(d) $(D, T) = (2.8, 1.2)$





n	Configuration	ΔE
1	○	$6J-D$
2	○—○	$11J-2D$
3	○—○ ○—○	$16J-3D$
4	○—○—○—○	$20J-4D$
	⋮	
8	○—○—○—○ ○—○—○—○ ○—○—○—○ ○—○—○—○	$36J-8D$
	⋮	
18	○—○—○—○—○—○—○—○—○ ○—○—○—○—○—○—○—○—○ ○—○—○—○—○—○—○—○—○ ○—○—○—○—○—○—○—○—○	$75J-18D$

